

Generate to Discriminate: Expert Routing for Continual Learning

Yewon Byun¹, Sanket Vaibhav Mehta¹, Saurabh Garg^{1,2}, Emma Strubell¹,
Michael Oberst³, Bryan Wilder¹, and Zachary C. Lipton¹

¹Carnegie Mellon University, ²Mistral AI, ³Johns Hopkins University

Abstract

In many real-world settings, regulations and economic incentives permit the sharing of models but not data across institutional boundaries. In such scenarios, practitioners might hope to adapt models to new domains, without losing performance on previous domains (so-called catastrophic forgetting). While any single model may struggle to achieve this goal, learning an ensemble of domain-specific experts offers the potential to adapt more closely to each individual institution. However, a core challenge in this context is determining which expert to deploy at test time. In this paper, we propose Generate to Discriminate (G2D), a domain-incremental continual learning method that leverages synthetic data to train a domain-discriminator that routes samples at inference time to the appropriate expert. Surprisingly, we find that leveraging synthetic data in this capacity is more effective than using the samples to *directly* train the downstream classifier (the more common approach to leveraging synthetic data in the lifelong learning literature). We observe that G2D outperforms competitive domain-incremental learning methods on tasks in both vision and language modalities, providing a new perspective on the use of synthetic data in the lifelong learning literature.

1 Introduction

To deploy machine learning reliably, it is important to develop methods for adapting models as we encounter environments sequentially in the wild. In medical imaging and risk prediction tasks, practitioners often apply models trained on one hospital’s data to make predictions on samples from other institutions [73, 48, 23]. Autonomous vehicle navigation systems must safely operate on different terrains, in different states, and even different countries. Moreover as we adapt to each new environment, it is desirable (whenever possible) that this adaptation comes without loss of accuracy in previously seen environments.

In such continual learning problems, some of the most effective methods rely on a rehearsal buffer to re-train on a portion of past samples [7, 39]. However, these solutions are often not viable in real-world prediction settings, where the landscape of regulatory and industry norms place stringent constraints on sharing data across institutional boundaries. We focus on the domain-incremental learning setting where the set of classes is fixed across domains and explicit data sharing across domains is prohibited. Crucially, domain identifiers are not given during inference time. The goal, after each round, is to produce a system that performs well on test examples drawn at random among all previously seen domains. At any round, our model only has access to the current data and, thus, simply performing gradient updates is liable to cause *catastrophic forgetting*, where performance decays on previously seen domains, even when the tasks are not fundamentally in conflict [43, 22]. To enable lifelong learning in scenarios characterized by stringent constraints on data sharing, several settings for this problem have been proposed [58]. For example, *generative replay* methods utilize generative models to create synthetic samples for experience rehearsal [55, 59, 49]. However, these approaches have largely under-performed state-of-the-art discriminative approaches [59], due at least in part to the introduction of noise in the form of low-quality synthetic data.

Without access to a rehearsal buffer, *rehearsal-free* methods often tackle forgetting with dynamically expandable systems with domain-specific parameters, such as expert models [2, 53] or parameter-efficient prompts [69, 68, 67]. As widely demonstrated in the literature [65, 67, 69], such modular approaches allow learning parameters independently across domains to potential negative interference, leading to

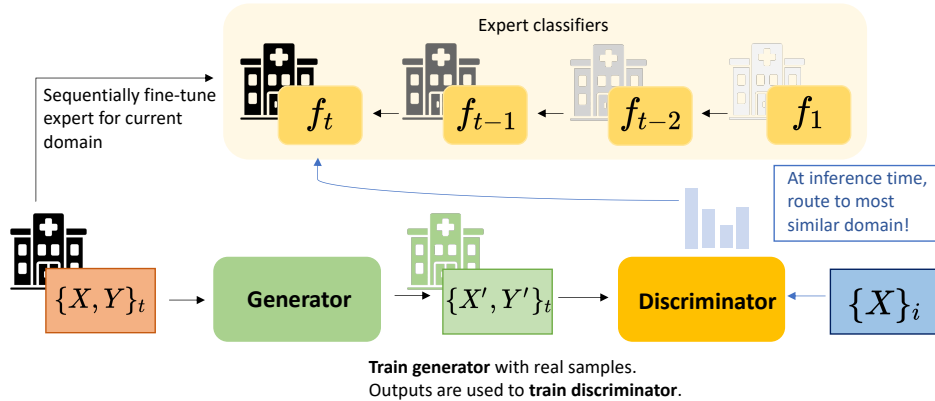


Figure 1: **Generate to Discriminate (G2D)**; During training (black text and arrows), we (i) finetune the generator and expert classifier and (ii) finetune a domain discriminator on synthetic images produced by our generator. At inference time (blue text and arrows), we route test samples to the corresponding expert, based on our discriminator’s prediction.

less/no forgetting and better transferring, avoiding tug-of-war scenarios that are exhibited in single, generalist models. However, a core remaining challenge is determining *which* expert or module to invoke at test time. Some recent methods rely on the implicit domain discriminative (zero-shot) capabilities of foundation models [1] for an inference-time routing strategy [67]. However, as we will show, in settings where the zero-shot discriminative performance of foundation models is limited, these methods underperform (see Table 1). The limitations and above-discussed challenges raise an interesting question: Rather than employing synthetic samples to train the downstream classifier, can synthetic samples serve a more effective purpose in domain discrimination? Can we leverage synthetically generated samples to develop an inference-time routing mechanism?

In this paper, we propose a simple yet effective method for expert routing in domain-incremental continual learning, *Generate to Discriminate (G2D)*. G2D leverages synthetic data to train a domain discriminator that routes inference-time samples to a set of domain-specific expert classifiers, each checkpointed after each domain is encountered. Surprisingly, we observe that using synthetic data for training a domain router is more effective than using the *same* samples to augment training data for training the label classifier (as in generative replay methods). We also find that our approach outperforms other competitive domain-incremental learning methods, such as replay, regularization-based, and rehearsal-free (prompt-based) methods across benchmarks in both vision and text modalities. To further stress test current methods in more realistic settings, we introduce a new benchmark, DermCL, which consists of a training sequence of four publicly available dermatology medical image classification tasks, each previously utilized independently to evaluate transfer learning or robustness to distribution shifts [71]. We empirically show that state-of-the-art prompt-based methods that rely on the implicit (zero-shot) capabilities of foundation models [1, 67] underperform (in comparison with our method) in these settings, where the downstream task (i.e., skin lesion prediction in minority populations) might diverge from tasks seen in pretraining corpora (see Table 1), emphasizing the need for more realistic benchmarks for a holistic evaluation of continual learning methods.

To summarize, our contributions are as follows:

- We empirically observe that with the *same* synthetic samples, training a domain identifier outperforms augmenting training data for the downstream label classifier—the common approach to leveraging synthetic data in the lifelong learning literature.
- Leveraging this observation, we develop a simple method for expert routing in the domain-incremental learning setting, without *any* access to real data from previously seen tasks, that outperforms considered baselines in both vision and text modalities.
- Towards evaluation of current methods in more realistic settings, we propose a new continual learning benchmark consisting of a sequence of four real-world, dermatology classification tasks.

2 Related Work

The majority of continual learning methods fall into (i) parameter-based and (ii) data-based regularization techniques [58]. We also touch upon more recent approaches, dubbed (iii) prompt-based techniques that leverage pretrained models.

Parameter-based Regularization Approaches. Most notable works in this category, namely Elastic Weight Consolidation (EWC; Kirkpatrick et al. [31]) and Synaptic Intelligence (SI; Zenke et al. [74]), assess the importance of parameters related to previous domains and use a penalty term to safeguard the knowledge stored in those parameters while updating them for new domains. Another work similarly preserves the knowledge of previous tasks by using the initial task knowledge as a regularizer during training [36].

Data-based Regularization Approaches. Several competitive methods in the literature retain a subset of data from previous domains as an episodic memory, which is sparsely replayed during the learning of new domains. Each differ in whether the episodic memory is utilized during training, such as GEM [39], A-GEM [6], ER [7], MEGA [24], or during inference, such as MbPA [13, 70]. These methods assume access to retaining true data from previous domains. Yet, this assumption is often violated in practice. Towards operating under more practical assumptions, deep generative replay-based methods have been introduced (DGR; Shin et al. [55], LAMOL; Sun et al. [59], LFPT5; Qin and Joty [49]), where generative models are used to generate synthetic samples for experience replay, often referred to as generative replay. However, these approaches have largely under-performed state-of-the-art discriminative approaches [59], due at least in part to the introduction of noise in the form of low-quality synthetic samples.

Prompt-based and Modular Approaches. Without access to a rehearsal buffer, *rehearsal-free* methods tackle forgetting with dynamically expandable systems with domain-specific parameters, such as expert models [2, 53, 34, 46] or parameter-efficient prompts [67, 68, 66, 32, 72].¹ The key challenge in such approaches is determining which expert or module to invoke at inference time. Some methods assume access to task identity at test time [12, 35, 65] or access to previous samples [15, 3]. However, these assumptions generally restrict practical use in settings where data sharing between institutions are prohibited. In response to the increasing popularity of pretrained models, recent methods rely on the implicit domain discriminative (zero-shot) capabilities of foundation models [1, 75] for an inference-time routing strategy [67]. Mehta et al. [44] demonstrates that pretrained initializations implicitly mitigate the issue of forgetting when sequentially finetuning models. A more recent line of work, known as prompt-based continual learning, exemplified by L2P [69], DualPrompt [68], S-Prompts [67], and CODA-Prompt [57], involves learning a small number of parameters per domain in the form of continuous token embeddings or prompts while keeping the remaining pretrained model fixed. Although such methods allow continual learning without rehearsal, they depend on access to pretrained models that provide a high-quality backbone across all domains, which may not be available in sensitive environments in real-world deployment (e.g., healthcare). While many methods have been proposed, it is unclear whether they will work well in real-world deployment settings when their implicit assumptions are violated.

3 Preliminaries

In domain-incremental continual learning, the primary goal is to learn a model that adapts to each new domain while mitigating catastrophic forgetting on previously seen domains [62]. Formally, we consider a sequence of T domains, $\mathcal{D}_1 \rightarrow \dots \rightarrow \mathcal{D}_T$, where $\mathcal{D}_t = \{x_i^t, y_i^t\}_{i=0}^{N_t}$ represents a dataset corresponding to domain t , sampled from an underlying distribution $P_t(\mathcal{X}, \mathcal{Y})$. $x_i^t \in \mathcal{X}$ is the i -th image or text passage and $y_i^t \in \mathcal{Y}$ is its label. N_t is the total number of samples for domain t . Under this premise, $\forall t$, the marginal or conditional distributions over \mathcal{X} and \mathcal{Y} can change, i.e., $P_t(\mathcal{X}) \neq P_{t+1}(\mathcal{X})$ and $P_t(\mathcal{Y}|\mathcal{X}) \neq P_{t+1}(\mathcal{Y}|\mathcal{X})$, while the label space \mathcal{Y} remains fixed across all domains. The goal is to learn a predictor $f_\theta : \mathcal{X} \rightarrow \mathcal{Y}$, a neural network parameterized by $\theta \in R^P$, to minimize the average expected

¹More broadly, modular approaches utilizing expert models have demonstrated effectiveness across various settings [76], including (but not limited to) multi-task learning [25, 21].

risk \hat{R}_T across all T domains

$$\hat{R}_T(f_\theta; \mathcal{D}_1, \dots, \mathcal{D}_T) = \frac{1}{T} \sum_{t=1}^T \frac{1}{N_t} \sum_{i=0}^{N_t} \ell(f_\theta(x_i^t), y_i^t), \quad (1)$$

where ℓ is a loss function. As standard in the literature, we take ℓ as the cross entropy loss.

Since the predictor f_θ only has access to the current data \mathcal{D}_t during each phase t of the training sequence, this prevents the direct minimization of the average expected risk (Equation 1). If a model sequentially trains by focusing only on minimizing the empirical risk of the current domain, it risks catastrophic forgetting of knowledge acquired from previous domains. Therefore, to demonstrate the model’s learning behavior over the sequence of domains and analyze catastrophic forgetting of the previously seen domains, we evaluate the model after training on a specific domain t using the test dataset of that domain, $\mathcal{D}_t^{test} \sim P_t(\mathcal{X}, \mathcal{Y})$, and all test datasets from previously seen domains, $\mathcal{D}_i^{test} \sim P_i(\mathcal{X}, \mathcal{Y}), \forall i \in [1, \dots, t-1]$. We remark that the domain identity is known only during sequential training and not during inference-time. The goal of domain-incremental continual learning is to produce a system that performs well on test samples randomly drawn from all previously seen domains. Let $\alpha_{s,t}$ denote the accuracy on domain s after training on domain t . Following prior work [39], we compute the *average accuracy* (A_t) metric after training on the domain t . This is given by

$$A_t = \frac{1}{t} \sum_{s=1}^t \alpha_{s,t}. \quad (2)$$

4 Generate to Discriminate (G2D)

Motivated by the limitations of previous works [55, 59, 49], rather than employing synthetic data to augment training data to train the downstream label classifier, we ask whether synthetic data can be used to develop an inference-time routing mechanism. Access to an accurate domain discriminator would answer the question of which expert or module to invoke at inference-time, without any access to real data or ground truth annotations from which domain each data is sourced. Alongside this domain discriminator (router), we learn and maintain a set of domain-specific experts, which we invoke during inference-time according to the router’s predictions. We refer to our method of using synthetic data to learn an expert routing mechanism as **Generate to Discriminate (G2D)**.

4.1 Generation of Synthetic Samples

At each domain \mathcal{D}_t , we finetune a generative model G with samples from the current domain $\{(x_i^t, y_i^t)\}_{i=0}^{N_t}$. For our generator for the vision domain, we finetune an off-the-shelf, text-to-image Stable Diffusion [52] model (see §C.1 for further details). For our generator for the text domain, we use a pretrained T5-Large v1.1 model [50] and optimize via prompt tuning [33], which learns continuous input token embeddings (see §B.1 and §C.2 for further details). After finetuning these models on each domain, we then sample synthetic examples \mathcal{M}_t from G , which will be used in our approach for learning an expert routing mechanism, as well as in the comparison to generative replay methods.

4.2 Training Expert Classifiers and the Routing Function

Given synthetically generated data from our generators on domains $\mathcal{D}_1, \dots, \mathcal{D}_t$, we finetune a domain discriminator (router), D_{θ_t} on the union of the synthetically generated samples $\mathcal{M}_1 \cup \dots \cup \mathcal{M}_{t-1} \cup \mathcal{M}_t$, for domain identity prediction (i.e., t -way classification). More formally, we construct a dataset of $\bigcup_{i=1}^t \{(x, i) | x \in \mathcal{M}_i\}$ to train a domain discriminator $D_{\theta_t} : \mathcal{X} \rightarrow \mathcal{Y}$, where $\mathcal{Y} = \{1, \dots, t-1, t\}$. In short, our domain discriminator learns to predict domain membership, or route samples to their corresponding or most similar domains.

At each domain \mathcal{D}_t , we finetune our classifier f_{θ_t} as the expert on domain t , and add f_{θ_t} to our list of experts $\{f_{\theta_1}, \dots, f_{\theta_{t-1}}, f_{\theta_t}\}$. At inference time, we use our domain discriminator to predict the most likely domain identity t , and the test sample is routed to the corresponding expert classifier f_{θ_t} for our final class prediction (see Figure 1 for a schematic visualization of our approach). For our expert classifiers and domain discriminator for the vision domain, we use a vision transformer (ViT B-16) [17]

pretrained on ImageNet [14]. For the text domain, we use a pretrained BERT-Base [29] backbone. To select our hyperparameters, we use the source hold-out performance to select the best combination of parameters (see §C.1 and §C.2 for further details).

5 Experimental Setup

We compare our approach to generative replay approaches and other domain-incremental approaches across a variety of domain-incremental learning benchmarks in both vision and text modalities.

5.1 Datasets and Metrics

For our vision experiments, we look at standard domain-incremental benchmarks: DomainNet [47] and CORe50 [38], and DermCL (see §5.1), our newly introduced benchmark curated from real-world dermatology tasks [60, 5, 45, 11]. We use the standard ordering for DomainNet: real, quickdraw, painting, sketch, infograph, and clipart. For CORe50, we use the standard setting of a sequence of 8 domains, with three fixed test domains that are out-of-distribution (OOD). On this task, we remark that learning a domain discriminator essentially learns a similarity function between domains and the OOD test example, routing each new example to the expert trained on the most similar in-distribution (ID) domain. For both datasets, we report average accuracy averaged over 5 random seeds.

For our text experiments, we evaluate our method on the standard domain-incremental question-answering (QA) benchmark as introduced in the work of de Masson D’Autume et al. [13]. The benchmark consists of three QA datasets: SQuAD v1.1[51], TriviaQA [27] and QuAC [9]. TriviaQA has two sections, Web and Wikipedia, which are considered as separate datasets. We use four different orderings of domain sequences (see §A.2). Following prior works [13, 70], we compute the F_1 score for the QA task and evaluate the model at the end of all domains, i.e., we compute A_4 .

DermCL Benchmark. The lack of realistic benchmarks in the continual learning community and the artificial temporal variation in existing benchmarks have been highlighted in the literature [38, 37, 68]. Towards a more holistic evaluation of existing methods on realistic variation in domain shifts, we propose a new continual learning benchmark (**DermCL**), which presents *real world distribution shifts* in dermoscopic images, due to differences in patient demographics, dataset collection period, camera types, and image quality. The benchmark spans four domains of dermoscopic image datasets – HAM10000 [60], BCN2000 [5], PAD-UEFS-20 [45], and DDI [11], for a classification task over 5 unified labels of skin lesions. Notably, DDI has been attributed to exhibiting a large performance drop, due to the presence of more dark skin tones from minority groups, exemplifying how failures of backward transfer (i.e., catastrophic forgetting) can have catastrophic outcomes. All four datasets in the sequence are publicly available (see §A.3 for details). We believe that this provides an important evaluation for modern domain-incremental learning approaches, as they often rely on large pretrained models that may have very different pretraining datasets from such real world tasks (e.g., medical imaging).

5.2 Baselines

Generative Replay. A common way to use synthetic data in lifelong learning is as a buffer of limited synthetic samples used to train the label classifier, introduced by Shin et al. [55], often referred to as Generative Replay. More precisely, at domain D_t , the generator G_t is finetuned with samples from the current domain $\{(x_i^t, y_i^t)\}_{i=0}^{N_t}$, generates synthetic samples \mathcal{M}_t from G_t , and stores these samples in a replay buffer. At domain D_{t+1} , the classifier f_θ is sequentially trained on the union of synthetic samples from previous domains $\bigcup_{i=1}^{t-1} \{(x, i) | x \in \mathcal{M}_i\}$ and real samples from the current domain $\{(x_i^t, y_i^t)\}_{i=0}^{N_t}$. We include specific implementation details in §B.2.

Other Baselines. First, we assess vanilla sequential finetuning (**SeqFT**), which does not employ any continual learning regularization techniques. Second, we compare with a traditional, parameter-based regularization method, elastic weight consolidation (**EWG**; 31). For vision experiments, we further compare with recent advances in prompt-based methods which have greatly boosted state-of-the-art performance across many vision benchmarks. Specifically, we compare our method with **L2P**; 69 and **S-Prompts** [67], as they exhibit competitive performance on domain-incremental learning tasks.²

²We note that there exist two variants of S-Prompts (ViT-based, and CLIP-based). For a fair comparison, we compare with the ViT-based variant that uses the same underlying pretrained checkpoint as the other baselines and G2D.

Table 1: Vision Results. For DomainNet and CORe50, we report performance in terms of average accuracy. For DermCL, performance is reported in terms of average AUC (due to high label imbalance). † denotes results obtained from Wang et al. [67]. For Experience Replay and Generative Replay, we use a fixed buffer size of 15/class for DomainNet and 100/class for DermCL, according to the lower bound on samples per class in the actual dataset; and 50/class for CORe50, following previous practice [70].

Method	DomainNet	CORe50	DermCL
Seq-FT	57.45 ± 0.36	83.10 ± 0.50	70.49 ± 2.51
EWC	57.25 ± 0.18	82.10 ± 1.89	75.26 ± 0.69
L2P	40.2 [†]	78.3 ± 0.1 [†]	74.20 ± 1.42
S-Prompts	56.13 ± 0.39	83.38 ± 0.36	81.59 ± 0.22
Generative Replay	60.16 ± 0.64	92.50 ± 0.40	81.23 ± 1.12
G2D (Ours)	70.03 ± 0.02	94.05 ± 0.53	85.24 ± 0.85
Oracle Router	71.24 ± 0.18	95.44 ± 0.11	91.92 ± 0.31
Experience Replay	65.64 ± 0.47	93.65 ± 0.60	89.17 ± 0.79
Upper Bound (MTL)	75.10 ± 0.09	97.19 ± 0.12	93.34 ± 0.96

Oracle and Quasi-Oracle Baselines. We also compare with the following *oracle* baselines. First, we compare against the setting of when access to real data from *all domains* is allowed at every task step, termed the multi-task learning (MTL) baseline. This is equivalent to training on the union of all existing data and can be viewed as an upper bound on performance (i.e., oracle performance) when there is no significant negative transfer between domains. Next, we compare against the following *quasi-oracle* baselines. We compare against a setting we term **Oracle Router**, where we have access to all real examples simultaneously in training the expert router (as opposed to ours in G2D trained via synthetic samples). We compare against **Experience Replay (ER)**; Chaudhry et al. [7]), a data-based regularization method, where the buffer retains limited *real* samples for previously seen domains. For both ER and Generative Replay, we follow the precedent set in the work of de Masson D’Autume et al. [13], retaining and sampling samples in proportion to the dataset sizes. In the text domain, we additionally compare our approach with methods that leverage replay buffers with real samples for task-specific test-time adaptation, namely Memory-based Parameter Adaptation++ (**MbPA++**) [13] and **Meta-MbPA** [70]. Meta-MbPA trains the model to attain a more suitable initialization for test-time adaptation and achieves the state-of-the-art performance on the Question-Answering benchmark. Note that our setup prevents access to real samples or domain identities from previous domains, making these oracle and quasi-oracle baselines like Experience Replay, MbPA++, Meta-MbPA, Oracle Gate, and MTL inapplicable in practice. However, we still include these baselines for a more comprehensive comparison to demonstrate how G2D performs against methods that (i) retain access to *real* samples from previous domains or (ii) assume access to ground-truth domain identity.

6 Results

We observe that G2D outperforms competitive methods in the considered vision and text benchmarks: DomainNet, CORe50, DermCL, and Question Answering (Table 1, 2). Notably, on datasets characterized by significant domain shifts that amplify negative backward transfer, such as DomainNet and DermCL,³ our method achieves substantial performance improvements. Additionally, G2D demonstrates strong out-of-distribution (OOD) performance compared to prior baselines, as evidenced by results on CORe50, where evaluation encompasses three OOD

Table 2: Text Results. Performance is reported in terms of average F_1 (averaged over 4 domain sequences). ‡ denotes results obtained from Wang et al. [70]. ER, MbPA++ and Meta-MbPA uses a buffer size of 1% actual samples.

Method	Question Answering
Seq-FT	56.6 ± 5.7
EWC	55.9 ± 3.7
Generative Replay	59.5 ± 0.9
G2D (Ours)	64.7 ± 0.2
Oracle Router	65.4 ± 0.0
Experience Replay	62.6 ± 1.4
MbPA++	61.9 ± 0.2 [‡]
Meta-MbPA	64.9 ± 0.3 [‡]
Upper Bound (MTL)	68.6 ± 0.0

³DomainNet contains highly heterogeneous domains, as highlighted by prior works [67]. DermCL exhibits substantial domain shifts, due to its inclusion of patient populations with diverse racial backgrounds and skin tones.

Table 3: We report the accuracy of domain discrimination (expert routing) for the considered baselines to complement the analysis presented in Figure 2 and §6.1. Note the oracle discriminator refers to a model trained on real samples, serving as the reference upper bound. “-” denotes not applicable.

Dataset	S-Prompts Disc.	G2D Disc. (ours)	Oracle Disc.
CORE50	90.81 ± 0.27	97.38 ± 0.93	98.94 ± 0.07
QA	-	94.5 ± 0.2	97.1 ± 0.0

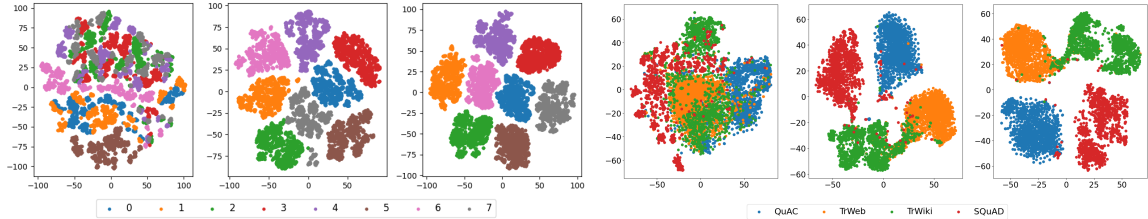


Figure 2: (Three left-most plots) Domain discrimination visualizations for CORE50 benchmark (8 domains). From left to right, the first subplot shows how domains are clustered via S-Prompts [67]. In the second and third subplots, the clusterings for our domain discriminator and the oracle discriminator are visualized. (Three right-most plots) Visualizations of domain clusterings for the QA benchmark (4 domains). The first subplot highlights the implicit domain discriminative nature of pretrained BERT-Base representations [29]. In the second and third subplots, we visualize the clustering of representations from our discriminator and the oracle discriminator trained using real samples. Interestingly, the discriminators trained with synthetic samples closely mirrors the performance and clustering patterns of the discriminators trained using real data.

datasets (e.g., domains never seen during training). Amongst the considered baselines, the comparison with Generative Replay is particularly instructive for understanding how to most effectively utilize synthetic data in the domain incremental learning setting. In this comparison, we examine two approaches (G2D, Generative Replay) that use the same set of synthetic samples, but in different ways.⁴ Our results demonstrate that using the same set of synthetic samples⁵ for domain discrimination consistently outperforms their use for augmenting training data for downstream classification (i.e., Generative Replay) across all considered benchmarks (see Table 1 and Table 2). Fundamentally, G2D relies on the generator to accurately model samples from different domains in order to train the domain discriminator. Generative Replay, on the other hand, requires an accurate modeling of downstream class labels rather than domains. Thus, our results empirically suggest that modeling the difference in domains is a relatively easier task than modeling the difference in downstream classes (for the considered generative models).

While our motivation to operate under more practical assumptions restricts data sharing across domains, we also include comparisons with competitive methods that assume access to real data from previously seen domains, for a more comprehensive evaluation. This allows us to understand the utility of our method even when such data constraints are relaxed. We observe that although our approach operates without access to real data from previously seen domains, it retains competitive performance with Experience Replay (see Table 1 and Table 2), and even outperforms the previous state-of-the-art in test-time adaptation-based continual learning, Meta-MbPA on text experiments (see Table 2). These findings underscore the ability of our method to enhance performance even in scenarios not characterized by stringent constraints on data sharing.

6.1 Analysis of Expert Routing Performance

To better understand our observed empirical gains, we examine our domain discriminator (expert router) independently from the overall pipeline. For this purpose, we make a departure from the downstream classification task and focus solely on analysis of the expert routing procedure.

⁴We include the specific details and implementation of Generative Replay in §B.2.

⁵In Table 11 and Figure 3 (see Appendix §F), we include example visualizations of generated samples for both modalities.

For the vision domain, we assess the performance of our discriminator with the (1) oracle discriminator (trained on a buffer of real samples) and (2) S-Prompts [67], a previous state-of-the-art domain incremental learning method that leverages a routing mechanism. S-Prompts leverages K-Means during training to store centroids for each domain; then during inference time, it employs KNN to identify the domain of a given test image feature by determining the domains of the K nearest centroids. In Figure 2, we present t-SNE plots [63] illustrating domain clusterings between these three methods for CORE50, the benchmark comprised of the longest domain sequence (eight domains). We observe that our method achieves more accurate clustering and domain identification than the S-Prompts method (see Table 3).

For the text domain, we present t-SNE plots visualizing the domain discriminative capability [1] of a pretrained language model and the G2D discriminator trained on synthetic samples (see Figure 2). Notably, in the pretrained language model’s clustering, there is confusion between the TrWeb (orange) and TrWiki (green) domains, both derived from the same TriviaQA dataset [27]. Similarly, the TrWiki (green) and SQuAD (red) domains, originating from the same Wikipedia source, necessitate explicit discriminator training. We clearly observe that training an explicit discriminator results in more accurate clustering. This is remedied in the clustering of the G2D discriminator, closely matching the behavior of the upper bound, namely a discriminator trained using real samples (see Table 3). Overall, for both vision and text domains, we observe that G2D improves domain identifiability (expert routing) and demonstrates competitive performance to a discriminator trained on *real* data, exhibiting similar clustering patterns.

7 Discussion, Limitations, and Conclusion

In this work, we propose a simple yet effective method for domain-incremental learning that leverages synthetic data to train a domain discriminator, enabling an inference-time routing mechanism. We establish that this approach is more effective than using the same synthetic samples to directly train the downstream label classifier (as past works have explored). While we do not claim that this phenomenon is universal, our findings consistently held true across many different domain-incremental learning benchmarks we investigated for both modalities. Further, our analysis on the capabilities of our domain discriminator, which encompasses existing domain discrimination approaches, unsupervised clustering methods, and a discriminator trained on real samples, finds that our method improves expert routing performance across both modalities. Building on this, expanded formulations of experts and modular architectures, such as mixture of experts [54] and its derivatives thereof (e.g., multi-gate mixture of experts [42]), offer intriguing possibilities for complementary extensions of our method, which we leave for future study. Motivated by our interest in real-world settings (e.g., clinical healthcare), where the prohibition on data sharing is especially well-motivated, and by the lack of realistic benchmarks in the continual learning community more broadly,⁶ we introduce a new domain-incremental learning benchmark to further stress-test competing methods. In addition to its practical relevance in the problem setting at hand, our observations provide interesting insights into different perspectives on the use of synthetic data in such scenarios where real data cannot be shared, which we leave for further study.

Limitations. A potential limitation of our method is that the number of experts scales linearly with the number of domains encountered. While this introduces potential computational overhead, it is unlikely to be prohibitive in our motivating scenarios (i.e., healthcare), where the number of domains (e.g., institutions) is typically modest, often on the order of tens. This ensures the method remains practical for real-world applications, though strategies to address scaling for larger domain counts warrant further exploration. Further, we remark that there exist potential privacy concerns, when leveraging generative models to sample synthetic data, where memorization could potentially reveal sensitive information from the original data in the training dataset. For these concerns, there is an important, separate field of work in improving the differential privacy [19, 20] of such methods, by training these models with privacy constraints [16, 41, 4]. In this work, we do not take a stand on when or whether the sharing of generative models (or synthetic samples) should be permissible. While this is an important issue to be considered prior to real-world deployment of any method that involves generative models, how institutional practices develop and how the regulatory environment evolves will be informed, to a large degree, by exploratory research that characterizes both (i) the potential benefits; and (ii) the potential risks associated with the dissemination of generative models trained on real data. We see our research as helping to elucidate the potential benefits of synthetic data in such settings.

⁶A problem often lamented in prior work [38, 37, 68]

Acknowledgments

We thank Praveer Singh and Jayashree Kalpathy-Cramer for valuable discussions on the practical challenges of domain incremental settings, particularly in healthcare applications. We thank Dylan Sam for thoughtful comments on the manuscript and experimental setup. We thank Alex Li and Brandon Trabucco for sharing helpful insights on diffusion models and synthetic data. YB was supported in part by the AI2050 program at Schmidt Sciences (Grant G-22-64474) and also gratefully acknowledges the NSF (IIS2211955), UPMC, Highmark Health, Abridge, Ford Research, Mozilla, the PwC Center, Amazon AI, JP Morgan Chase, the Block Center, the Center for Machine Learning and Health, and the CMU Software Engineering Institute (SEI) via Department of Defense contract FA8702-15-D-0002, for their generous support of ACMI Lab’s research.

References

- [1] Roei Aharoni and Yoav Goldberg. Unsupervised domain clusters in pretrained language models. In *Proceedings of the 58th Annual Meeting of the Association for Computational Linguistics*, pages 7747–7763, 2020.
- [2] Rahaf Aljundi, Punarjay Chakravarty, and Tinne Tuytelaars. Expert gate: Lifelong learning with a network of experts. In *Proceedings of the IEEE conference on computer vision and pattern recognition*, pages 3366–3375, 2017.
- [3] Vladimir Araujo, Marie-Francine Moens, and Tinne Tuytelaars. Learning to route for dynamic adapter composition in continual learning with language models. *arXiv preprint arXiv:2408.09053*, 2024.
- [4] Tianshi Cao, Alex Bie, Arash Vahdat, Sanja Fidler, and Karsten Kreis. Don’t generate me: Training differentially private generative models with sinkhorn divergence. *Advances in Neural Information Processing Systems*, 34:12480–12492, 2021.
- [5] Bill Cassidy, Connah Kendrick, Andrzej Brodzicki, Joanna Jaworek-Korjakowska, and Moi Hoon Yap. Analysis of the isic image datasets: Usage, benchmarks and recommendations. *Medical image analysis*, 75:102305, 2022.
- [6] Arslan Chaudhry, Marc’Aurelio Ranzato, Marcus Rohrbach, and Mohamed Elhoseiny. Efficient lifelong learning with a-GEM. In *International Conference on Learning Representations*, 2019.
- [7] Arslan Chaudhry, Marcus Rohrbach, Mohamed Elhoseiny, Thalaiyasingam Ajanthan, Puneet K Dokania, Philip HS Torr, and Marc’Aurelio Ranzato. On tiny episodic memories in continual learning. *arXiv preprint arXiv:1902.10486*, 2019.
- [8] Richard J Chen, Ming Y Lu, Tiffany Y Chen, Drew FK Williamson, and Faisal Mahmood. Synthetic data in machine learning for medicine and healthcare. *Nature Biomedical Engineering*, 5(6):493–497, 2021.
- [9] Eunsol Choi, He He, Mohit Iyyer, Mark Yatskar, Wen-tau Yih, Yejin Choi, Percy Liang, and Luke Zettlemoyer. Quac: Question answering in context. In *Proceedings of the 2018 Conference on Empirical Methods in Natural Language Processing*, pages 2174–2184, 2018.
- [10] Aaron S Coyner, Jimmy S Chen, Ken Chang, Praveer Singh, Susan Ostmo, RV Paul Chan, Michael F Chiang, Jayashree Kalpathy-Cramer, J Peter Campbell, Imaging, Informatics in Retinopathy of Prematurity Consortium, et al. Synthetic medical images for robust, privacy-preserving training of artificial intelligence: application to retinopathy of prematurity diagnosis. *Ophthalmology Science*, 2(2):100126, 2022.
- [11] Roxana Daneshjou, Kailas Vodrahalli, Roberto A Novoa, Melissa Jenkins, Weixin Liang, Veronica Rotemberg, Justin Ko, Susan M Swetter, Elizabeth E Bailey, Olivier Gevaert, et al. Disparities in dermatology ai performance on a diverse, curated clinical image set. *Science advances*, 8(31): eabq6147, 2022.

- [12] Matthias De Lange, Rahaf Aljundi, Marc Masana, Sarah Parisot, Xu Jia, Aleš Leonardis, Gregory Slabaugh, and Tinne Tuytelaars. A continual learning survey: Defying forgetting in classification tasks. *IEEE transactions on pattern analysis and machine intelligence*, 44(7):3366–3385, 2021.
- [13] Cyprien de Masson D’Autume, Sebastian Ruder, Lingpeng Kong, and Dani Yogatama. Episodic memory in lifelong language learning. *Advances in Neural Information Processing Systems*, 32, 2019.
- [14] Jia Deng, Wei Dong, Richard Socher, Li-Jia Li, Kai Li, and Li Fei-Fei. Imagenet: A large-scale hierarchical image database. In *2009 IEEE conference on computer vision and pattern recognition*, pages 248–255. Ieee, 2009.
- [15] Thang Doan, Seyed Iman Mirzadeh, and Mehrdad Farajtabar. Continual learning beyond a single model. In *Conference on Lifelong Learning Agents*, pages 961–991. PMLR, 2023.
- [16] Tim Dockhorn, Tianshi Cao, Arash Vahdat, and Karsten Kreis. Differentially private diffusion models. *arXiv preprint arXiv:2210.09929*, 2022.
- [17] Alexey Dosovitskiy, Lucas Beyer, Alexander Kolesnikov, Dirk Weissenborn, Xiaohua Zhai, Thomas Unterthiner, Mostafa Dehghani, Matthias Minderer, Georg Heigold, Sylvain Gelly, et al. An image is worth 16x16 words: Transformers for image recognition at scale. *arXiv preprint arXiv:2010.11929*, 2020.
- [18] August DuMont Schütte, Jürgen Hetzel, Sergios Gatidis, Tobias Hepp, Benedikt Dietz, Stefan Bauer, and Patrick Schwab. Overcoming barriers to data sharing with medical image generation: a comprehensive evaluation. *NPJ digital medicine*, 4(1):141, 2021.
- [19] Cynthia Dwork and Aaron Roth. *The Algorithmic Foundations of Differential Privacy*. Now Publishers Inc., 2014.
- [20] Cynthia Dwork, Frank McSherry, Kobbi Nissim, and Adam Smith. Calibrating noise to sensitivity in private data analysis. In *Theory of Cryptography Conference*, pages 265–284. Springer, 2006.
- [21] Zhiwen Fan, Rishov Sarkar, Ziyu Jiang, Tianlong Chen, Kai Zou, Yu Cheng, Cong Hao, Zhangyang Wang, et al. M³vit: Mixture-of-experts vision transformer for efficient multi-task learning with model-accelerator co-design. *Advances in Neural Information Processing Systems*, 35:28441–28457, 2022.
- [22] Robert M French. Catastrophic forgetting in connectionist networks. *Trends in cognitive sciences*, 3(4):128–135, 1999.
- [23] Hao Guan and Mingxia Liu. Domain adaptation for medical image analysis: a survey. *IEEE Transactions on Biomedical Engineering*, 69(3):1173–1185, 2021.
- [24] Yunhui Guo, Mingrui Liu, Tianbao Yang, and Tajana Rosing. Improved schemes for episodic memory-based lifelong learning. *Advances in Neural Information Processing Systems*, 33:1023–1035, 2020.
- [25] Hussein Hazimeh, Zhe Zhao, Aakanksha Chowdhery, Maheswaran Sathiamoorthy, Yihua Chen, Rahul Mazumder, Lichan Hong, and Ed Chi. Dselect-k: Differentiable selection in the mixture of experts with applications to multi-task learning. *Advances in Neural Information Processing Systems*, 34:29335–29347, 2021.
- [26] Edward J Hu, Yelong Shen, Phillip Wallis, Zeyuan Allen-Zhu, Yuanzhi Li, Shean Wang, Lu Wang, and Weizhu Chen. Lora: Low-rank adaptation of large language models. *arXiv preprint arXiv:2106.09685*, 2021.
- [27] Mandar Joshi, Eunsol Choi, Daniel Weld, and Luke Zettlemoyer. Triviaqa: A large scale distantly supervised challenge dataset for reading comprehension. In *Proceedings of the 55th Annual Meeting of the Association for Computational Linguistics (Volume 1: Long Papers)*, pages 1601–1611, 2017.
- [28] Fahad Kamran, Shengpu Tang, Erkin Otles, Dustin S McEvoy, Sameh N Saleh, Jen Gong, Benjamin Y Li, Sayon Dutta, Xinran Liu, Richard J Medford, et al. Early identification of patients admitted to hospital for covid-19 at risk of clinical deterioration: model development and multisite external validation study. *bmj*, 376, 2022.

- [29] Jacob Devlin Ming-Wei Chang Kenton and Lee Kristina Toutanova. Bert: Pre-training of deep bidirectional transformers for language understanding. In *Proceedings of NAACL-HLT*, pages 4171–4186, 2019.
- [30] Diederik P Kingma and Jimmy Ba. Adam: A Method for Stochastic Optimization. *arXiv Preprint arXiv:1412.6980*, 2014.
- [31] James Kirkpatrick, Razvan Pascanu, Neil Rabinowitz, Joel Veness, Guillaume Desjardins, Andrei A. Rusu, Kieran Milan, John Quan, Tiago Ramalho, Agnieszka Grabska-Barwinska, Demis Hassabis, Claudia Clopath, Dharshan Kumaran, and Raia Hadsell. Overcoming catastrophic forgetting in neural networks. *Proceedings of the National Academy of Sciences*, 114(13):3521–3526, mar 2017. doi: 10.1073/pnas.1611835114. URL <https://doi.org/10.1073/pnas.1611835114>.
- [32] Minh Le, An Nguyen, Huy Nguyen, Trang Nguyen, Trang Pham, Linh Van Ngo, and Nhat Ho. Mixture of experts meets prompt-based continual learning. *arXiv preprint arXiv:2405.14124*, 2024.
- [33] Brian Lester, Rami Al-Rfou, and Noah Constant. The power of scale for parameter-efficient prompt tuning. In *Proceedings of the 2021 Conference on Empirical Methods in Natural Language Processing*, pages 3045–3059, 2021.
- [34] Hongbo Li, Sen Lin, Lingjie Duan, Yingbin Liang, and Ness B Shroff. Theory on mixture-of-experts in continual learning. *arXiv preprint arXiv:2406.16437*, 2024.
- [35] Xilai Li, Yingbo Zhou, Tianfu Wu, Richard Socher, and Caiming Xiong. Learn to grow: A continual structure learning framework for overcoming catastrophic forgetting. In *International conference on machine learning*, pages 3925–3934. PMLR, 2019.
- [36] Zhizhong Li and Derek Hoiem. Learning without forgetting. *IEEE transactions on pattern analysis and machine intelligence*, 40(12):2935–2947, 2017.
- [37] Zhiqiu Lin, Jia Shi, Deepak Pathak, and Deva Ramanan. The clear benchmark: Continual learning on real-world imagery. In *Thirty-fifth conference on neural information processing systems datasets and benchmarks track (round 2)*, 2021.
- [38] Vincenzo Lomonaco and Davide Maltoni. Core50: a new dataset and benchmark for continuous object recognition. In *Conference on robot learning*, pages 17–26. PMLR, 2017.
- [39] David Lopez-Paz and Marc’Aurelio Ranzato. Gradient episodic memory for continual learning. *Advances in neural information processing systems*, 30, 2017.
- [40] Ilya Loshchilov and Frank Hutter. Decoupled weight decay regularization. *arXiv preprint arXiv:1711.05101*, 2017.
- [41] Saiyue Lyu, Margarita Vinaroz, Michael F Liu, and Mijung Park. Differentially private latent diffusion models. *arXiv preprint arXiv:2305.15759*, 2023.
- [42] Jiaqi Ma, Zhe Zhao, Xinyang Yi, Jilin Chen, Lichan Hong, and Ed H Chi. Modeling task relationships in multi-task learning with multi-gate mixture-of-experts. In *Proceedings of the 24th ACM SIGKDD international conference on knowledge discovery & data mining*, pages 1930–1939, 2018.
- [43] Michael McCloskey and Neal J Cohen. Catastrophic interference in connectionist networks: The sequential learning problem. In *Psychology of learning and motivation*, volume 24, pages 109–165. Elsevier, 1989.
- [44] Sanket Vaibhav Mehta, Darshan Patil, Sarath Chandar, and Emma Strubell. An empirical investigation of the role of pre-training in lifelong learning. *Journal of Machine Learning Research*, 24(214):1–50, 2023. URL <http://jmlr.org/papers/v24/22-0496.html>.
- [45] Andre GC Pacheco, Gustavo R Lima, Amanda S Salomao, Breno Krohling, Igor P Biral, Gabriel G de Angelo, Fábio CR Alves Jr, José GM Esgario, Alana C Simora, Pedro BC Castro, et al. Pad-ufes-20: A skin lesion dataset composed of patient data and clinical images collected from smartphones. *Data in brief*, 32:106221, 2020.

- [46] Sejik Park. Learning more generalized experts by merging experts in mixture-of-experts. *arXiv preprint arXiv:2405.11530*, 2024.
- [47] Xingchao Peng, Qinxun Bai, Xide Xia, Zijun Huang, Kate Saenko, and Bo Wang. Moment matching for multi-source domain adaptation. In *Proceedings of the IEEE/CVF international conference on computer vision*, pages 1406–1415, 2019.
- [48] Eduardo HP Pooch, Pedro Ballester, and Rodrigo C Barros. Can we trust deep learning based diagnosis? the impact of domain shift in chest radiograph classification. In *Thoracic Image Analysis: Second International Workshop, TIA 2020, Held in Conjunction with MICCAI 2020, Lima, Peru, October 8, 2020, Proceedings 2*, pages 74–83. Springer, 2020.
- [49] Chengwei Qin and Shafiq Joty. LFPT5: A unified framework for lifelong few-shot language learning based on prompt tuning of t5. In *International Conference on Learning Representations*, 2022.
- [50] Colin Raffel, Noam Shazeer, Adam Roberts, Katherine Lee, Sharan Narang, Michael Matena, Yanqi Zhou, Wei Li, and Peter J Liu. Exploring the limits of transfer learning with a unified text-to-text transformer. *The Journal of Machine Learning Research*, 21(1):5485–5551, 2020.
- [51] Pranav Rajpurkar, Jian Zhang, Konstantin Lopyrev, and Percy Liang. Squad: 100,000+ questions for machine comprehension of text. In *Proceedings of the 2016 Conference on Empirical Methods in Natural Language Processing*, pages 2383–2392, 2016.
- [52] Robin Rombach, Andreas Blattmann, Dominik Lorenz, Patrick Esser, and Björn Ommer. High-resolution image synthesis with latent diffusion models. In *Proceedings of the IEEE/CVF conference on computer vision and pattern recognition*, pages 10684–10695, 2022.
- [53] Grzegorz Rypeść, Sebastian Cygert, Valeriya Khan, Tomasz Trzciński, Bartosz Zieliński, and Bartłomiej Twardowski. Divide and not forget: Ensemble of selectively trained experts in continual learning. *arXiv preprint arXiv:2401.10191*, 2024.
- [54] Noam Shazeer, Azalia Mirhoseini, Krzysztof Maziarz, Andy Davis, Quoc Le, Geoffrey Hinton, and Jeff Dean. Outrageously large neural networks: The sparsely-gated mixture-of-experts layer. *arXiv preprint arXiv:1701.06538*, 2017.
- [55] Hanul Shin, Jung Kwon Lee, Jaehong Kim, and Jiwon Kim. Continual learning with deep generative replay. *Advances in neural information processing systems*, 30, 2017.
- [56] James Seale Smith, Yen-Chang Hsu, Lingyu Zhang, Ting Hua, Zolt Kira, Yilin Shen, and Hongxia Jin. Continual diffusion: Continual customization of text-to-image diffusion with c-lora. *arXiv preprint arXiv:2304.06027*, 2023.
- [57] James Seale Smith, Leonid Karlinsky, Vyshnavi Gutta, Paola Cascante-Bonilla, Donghyun Kim, Assaf Arbelle, Rameswar Panda, Rogerio Feris, and Zolt Kira. Coda-prompt: Continual decomposed attention-based prompting for rehearsal-free continual learning. In *Proceedings of the IEEE/CVF Conference on Computer Vision and Pattern Recognition*, pages 11909–11919, 2023.
- [58] Shagun Sodhani, Mojtaba Faramarzi, Sanket Vaibhav Mehta, Pranshu Malviya, Mohamed Abdelsalam, Janarthanan Janarthanan, and Sarath Chandar. An introduction to lifelong supervised learning. *arXiv preprint arXiv:2207.04354*, 2022.
- [59] Fan-Keng Sun, Cheng-Hao Ho, and Hung-Yi Lee. {LAMAL}: {LA}nguage modeling is all you need for lifelong language learning. In *International Conference on Learning Representations*, 2020.
- [60] Philipp Tschandl, Cliff Rosendahl, and Harald Kittler. The ham10000 dataset, a large collection of multi-source dermatoscopic images of common pigmented skin lesions. *Scientific data*, 5(1):1–9, 2018.
- [61] Alvaro E Ulloa-Cerna, Linyuan Jing, John M Pfeifer, Sushravya Raghunath, Jeffrey A Ruhl, Daniel B Rocha, Joseph B Leader, Noah Zimmerman, Greg Lee, Steven R Steinhubl, et al. Rechommend: an ecg-based machine learning approach for identifying patients at increased risk of undiagnosed structural heart disease detectable by echocardiography. *Circulation*, 146(1):36–47, 2022.

- [62] Gido M Van de Ven and Andreas S Tolias. Three scenarios for continual learning. *arXiv preprint arXiv:1904.07734*, 2019.
- [63] Laurens Van der Maaten and Geoffrey Hinton. Visualizing data using t-sne. *Journal of machine learning research*, 9(11), 2008.
- [64] Colin G Walsh, Michael A Ripperger, Yirui Hu, Yi-han Sheu, Drew Wilimitis, Amanda B Zheutlin, Daniel Rocha, Karmel W Choi, Victor M Castro, H Lester Kirchner, et al. Development and multi-site external validation of a generalizable risk prediction model for bipolar disorder. *medRxiv*, pages 2023–02, 2023.
- [65] Liyuan Wang, Xingxing Zhang, Qian Li, Jun Zhu, and Yi Zhong. Coscl: Cooperation of small continual learners is stronger than a big one. In *European Conference on Computer Vision*, pages 254–271. Springer, 2022.
- [66] Liyuan Wang, Jingyi Xie, Xingxing Zhang, Mingyi Huang, Hang Su, and Jun Zhu. Hierarchical decomposition of prompt-based continual learning: Rethinking obscured sub-optimality. *Advances in Neural Information Processing Systems*, 36, 2024.
- [67] Yabin Wang, Zhiwu Huang, and Xiaopeng Hong. S-prompts learning with pre-trained transformers: An occam’s razor for domain incremental learning. In Alice H. Oh, Alekh Agarwal, Danielle Belgrave, and Kyunghyun Cho, editors, *Advances in Neural Information Processing Systems*, 2022. URL https://openreview.net/forum?id=ZVe_WeMold.
- [68] Zifeng Wang, Zizhao Zhang, Sayna Ebrahimi, Ruoxi Sun, Han Zhang, Chen-Yu Lee, Xiaoqi Ren, Guolong Su, Vincent Perot, Jennifer Dy, et al. Dualprompt: Complementary prompting for rehearsal-free continual learning. In *European Conference on Computer Vision*, pages 631–648. Springer, 2022.
- [69] Zifeng Wang, Zizhao Zhang, Chen-Yu Lee, Han Zhang, Ruoxi Sun, Xiaoqi Ren, Guolong Su, Vincent Perot, Jennifer Dy, and Tomas Pfister. Learning to prompt for continual learning. In *Proceedings of the IEEE/CVF Conference on Computer Vision and Pattern Recognition*, pages 139–149, 2022.
- [70] Zirui Wang, Sanket Vaibhav Mehta, Barnabás Póczós, and Jaime G Carbonell. Efficient meta lifelong-learning with limited memory. In *Proceedings of the 2020 Conference on Empirical Methods in Natural Language Processing (EMNLP)*, pages 535–548, 2020.
- [71] Kathryn Wantlin, Chenwei Wu, Shih-Cheng Huang, Oishi Banerjee, Farah Dadabhoy, Veeral Vipin Mehta, Ryan Wonhee Han, Fang Cao, Raja R Narayan, Errol Colak, et al. Benchmd: A benchmark for modality-agnostic learning on medical images and sensors. *arXiv preprint arXiv:2304.08486*, 2023.
- [72] Jiazuo Yu, Yunzhi Zhuge, Lu Zhang, Ping Hu, Dong Wang, Huchuan Lu, and You He. Boosting continual learning of vision-language models via mixture-of-experts adapters. In *Proceedings of the IEEE/CVF Conference on Computer Vision and Pattern Recognition*, pages 23219–23230, 2024.
- [73] John R Zech, Marcus A Badgeley, Manway Liu, Anthony B Costa, Joseph J Titano, and Eric Karl Oermann. Variable generalization performance of a deep learning model to detect pneumonia in chest radiographs: a cross-sectional study. *PLoS medicine*, 15(11):e1002683, 2018.
- [74] Friedemann Zenke, Ben Poole, and Surya Ganguli. Continual learning through synaptic intelligence. In *International conference on machine learning*, pages 3987–3995. PMLR, 2017.
- [75] Da-Wei Zhou, Hai-Long Sun, Jingyi Ning, Han-Jia Ye, and De-Chuan Zhan. Continual learning with pre-trained models: A survey. *arXiv preprint arXiv:2401.16386*, 2024.
- [76] Yanqi Zhou, Tao Lei, Hanxiao Liu, Nan Du, Yanping Huang, Vincent Zhao, Andrew M Dai, Quoc V Le, James Laudon, et al. Mixture-of-experts with expert choice routing. *Advances in Neural Information Processing Systems*, 35:7103–7114, 2022.

A Dataset Details

In this section, we provide additional details about the datasets used in our experiments. We provide the overall dataset statistics in Table 4.

A.1 Overall Dataset Statistics

Table 4: Per-domain statistics for the continual learning benchmarks used in both vision and text experiments.

Dataset	Domain	Train	Validation	Test
CORe50 [38]	0	13491	1499	44972
	1	13495	1500	44972
	2	13487	1499	44972
	3	13494	1499	44972
	4	13490	1499	44972
	5	13490	1499	44972
	6	13469	1497	44972
	7	13485	1498	44972
DomainNet [47]	Real	108814	12091	52040
	Quickdraw	108674	12075	51749
	Painting	45373	5041	21849
	Sketch	43389	4821	20915
	Infograph	32419	3602	15581
	Clipart	30171	3352	14603
DermCL	HAM10000 [60]	7210	802	2003
	BCN2000 [5]	18238	2027	5066
	PAD-UEFS-20 [45]	1655	184	459
	DDI [11]	419	105	132
Question Answering [13]	SQuAD 1.1 [51]	81000	9000	10000
	TriviaQA (Web) [27]	68400	7600	10000
	TriviaQA (Wiki) [27]	54000	6000	8000
	QuAC [9]	72000	8000	7000

A.2 Question Answering Task Orders

For our Question-Answering (QA) benchmark[13], we consider the following four sequences of dataset orderings for a more comprehensive evaluation. We report the average accuracy over all sequences.

1. QuAC \rightarrow TriviaQA (Web) \rightarrow TriviaQA (Wiki) \rightarrow SQuAD
2. SQuAD \rightarrow TriviaQA (Wiki) \rightarrow QuAC \rightarrow TriviaQA (Web)
3. TriviaQA (Web) \rightarrow TriviaQA (Wiki) \rightarrow SQuAD \rightarrow QuAC
4. TriviaQA (Wiki) \rightarrow QuAC \rightarrow TriviaQA (Web) \rightarrow SQuAD

A.3 DermCL Benchmark Details

This benchmark offers a sequence of four dermatology imaging tasks. Distribution shifts are present across all four domains (HAM10000[60], BCN2000[5], PAD-UEFS-20[45], and, DDI[11]), in both demographics and data collection techniques. Dermoscopic image classification on diverse patient populations present complexities arising from (but not limited to) intraclass variations encompassing lesion texture, scale, and color. The label space for DermCL is defined as the following 5 unified labels: MEL (melanoma), NEV (nevus), BCC (basal cell carcinoma), AKIEC (includes actinic keratoses, intraepithelial carcinoma, squamous cell carcinoma), and Other diseases. We provide additional details about each domain in the following Table 5. All four datasets in the sequence are publicly available at

<https://github.com/rajpurkarlab/BenchMD> [71] (for HAM10000, BCN2000, PAD-UEFS-20) and <https://ddi-dataset.github.io> [11] (for DDI).

Table 5: Per-domain information for the DermCL Benchmark.

Domain	Description
HAM10000[60]	The HAM10000 dataset was collected over the past 20 years from hospitals in Austria and Australia using dermatoscopes.
BCN2000[5]	The BCN2000 dataset was collected from Spanish hospitals between 2010 and 2016 using dermatoscopes.
PAD-UEFS-20[45]	The PAD-UEFS-20 dataset was collected from Brazilian hospitals in 2020 using smartphone cameras.
DDI[11]	The DDI dataset contains images collected from pathology reports in Stanford Clinics from 2010-2020, representing 570 unique patients with diverse skin tone representation. It is notable for inducing significant performance drops in models, due to the presence of more dark skin tones and uncommon diseases.

B Additional Implementation Details

In this section, we provide additional details about the (1) implementation of our method, (2) implementation of generative replay, (3) computational costs, and (4) hardware requirements.

B.1 G2D Implementation Details

Vision. For our generator, we use an off-the-shelf, text-to-image Stable Diffusion [52] for our generative model (see Appendix §C.1 for further hyperparameter details). During inference, we prompt the text-to-image conditional diffusion model with the text label to sample generations. For our expert classifiers and domain discriminator, we use a Vision Transformer (ViT B-16) [17], initialized with the pretrained ImageNet [14] checkpoint. For our hyperparameter search, we use the source hold-out performance to select the best combination of parameters (see Appendix §C.1 for further details). For parameter efficiency, we finetune our expert classifiers with low-rank adaptation (i.e., LoRA) [26], where we only adapt the attention weights and keep the remaining parameters of the UNet architecture frozen.

Text. For our generator, we use prompt tuning to learn the parameter-efficient models [33]. We use the pretrained T5-Large v1.1 checkpoint adapted for prompt tuning as the backbone [50] and the prompt embeddings are initialized randomly. We input a special token into the model and conditionally generate a document content, question, and answer, all separated by the special tokens. During the generation process, we provide multiple text prompts. We use the following text prompts to conditionally generate synthetic samples:

```

text_prompts = [
    "Generate article, question and answer.",
    "Generate context, question and answer.",
    "Generate answers by copying from the generated article.",
    "Generate factual questions from the generated article."
]

```

During generation, we use ancestral sampling, which selects the next token randomly based on the model’s probability distribution over the entire vocabulary, thereby reducing the risk of repetition. We generate samples with a minimum length of 50 tokens and a maximum of 1,000 tokens and retain only those samples that contain exactly one question-answer pair with the answer included in the generated document content. For training our domain discriminator and expert classifiers, we use low-rank adaptation (LoRA; 26) and freeze the pretrained BERT-Base [29] backbone (see Appendix §C.2 for further details).

B.2 Generative Replay Implementation Details

We implement Generative Replay following standard practice [55] with the following updates to address limitations of the original approach: (1) The generative model originally used by Shin et al. [55], WGAN-GP, is quite outdated. To ensure a fair comparison, we revisit Generative Replay using the same generative models employed in our method (G2D) — Stable Diffusion [52] for vision data and T5 [50] for text data. (2) In the original Generative Replay implementation, the generator is sequentially finetuned (in addition to the classifier) on each domain in the sequence. This introduces the challenge of catastrophic forgetting in the generative model and introduces additional artifacts caused by continually training on noisy samples. In order to address this issue, there is an important line of work [56] focused on investigating catastrophic forgetting *within the learning procedure of generative models*, but such investigations fall beyond the scope of this study. Instead, for the purposes of this work, we mitigate this issue by finetuning the generator from the pretrained checkpoint rather than the finetuned checkpoint from the previous domain. This is applied consistently to both G2D and Generative Replay to ensure a fair comparison. In summary, these adjustments allow us to compare the performance of Generative Replay with our method, ensuring both approaches utilize the **same fixed set of synthetic samples**.

B.3 Computational Cost

We elaborate on details regarding the computational cost of our method, relative to naive expert learning: Our method incurs an additional total of 6-8 hours of computational cost on a single A6000 GPU, due to finetuning and sampling from the generator. Training the task discriminator, which takes less than 1-3 hours is done in parallel with training the expert classifier, so given that we permit the use of one more GPU, it does not incur additional compute time.

B.4 Hardware Requirements

All experiments were conducted using NVIDIA RTX A6000 and NVIDIA RTX 6000Ada graphics cards.

C Hyperparameter Details

C.1 Vision Experiment Hyperparameter Details

For all of our baselines, experts, and domain discriminators, we use the same pretrained model checkpoints, namely, the ViT-B/16 checkpoint trained on ImageNet (`vit_base_patch16_224`), released by Pytorch Image Models (timm). For our generative model, we use Stable Diffusion [52] as our conditional diffusion model with weights from the CompVis/stable-diffusion-v1-4 checkpoint. Hyperparameters are detailed in Table 6 and Table 7. For all hyperparameter searches, we use the source hold-out performance to select the best combination of parameters.

Table 6: Finetuning hyperparameters for the generative models in our vision experiments.

Hyperparameter	Value
Number of steps	150,000
Resolution	512
Learning Rate	$1e^{-5}$
Learning Rate Scheduler	Constant
Optimizer	AdamW [40]
Batch Size	16
Weight Decay	$1e^{-2}$

To ensure that we are evaluating our baselines comprehensively, we also run a hyperparameter search for different regularization values $\lambda \in [0.5, 1, 10, 100]$ for the Elastic Weight Consolidation (EWC) method, and use $\lambda = 1$. For Experience Replay and Generative Replay baselines, we retain (or sample) 15/class samples for DomainNet and 100/class samples for DermCL, according to the lower bound on samples per class in the actual dataset; and 50/class samples for CORE50, following previous practice [70]. For all of our baselines, we use the same pretrained model checkpoints, namely, the ViT-B/16 checkpoint trained on ImageNet (`vit_base_patch16_224`), released by Pytorch Image Models (timm).

Table 7: Finetuning hyperparameters for the classifiers in our vision experiments

Hyperparameter	DomainNet	CORe50	DermCL
Number of Epochs	20 ~ 50	10	10
Learning Rate	0.005 ~ 0.01	0.07	0.005
Optimizer	SGD	SGD	SGD
Momentum	0	0	0.9
Batch Size	128	128	128
LoRA Rank	16	16	16
LoRA Alpha	16	16	16

C.2 Text Experiment Hyperparameter Details

For our expert classifiers and domain discriminator, we use LoRA and freeze the pretrained BERT-Base [29] backbone. The BERT-base architecture has 12 Transformer layers, 12 self-attention heads, and 768 hidden dimensions (110M parameters). For our generative model, we use prompt tuning to learn parameter-efficient models [33]. We use the pretrained T5-Large v1.1 checkpoint adapted for prompt tuning as the backbone [50], and the prompt embeddings are initialized randomly. Hyperparameters are detailed in Table 8 and Table 9. The hyperparameters for baseline methods are set as described in Wang et al. [70]. For Experience Replay (and Generative Replay), we retain (or sample) 1% of examples which account for around 6,000 examples across all four considered domains.

Table 8: Finetuning hyperparameters for the generative models in our text experiments. We set the prompt length to 400 tokens as our prompt length, which accounts for 819k trainable parameters (roughly 0.1% of the total number of parameters in T5-Large). For our learning rate scheduler, we use warmup ratio of 0.01 and linear decay over 5 epochs.

Hyperparameters	Value
Prompt Length (Tokens)	400
Optimizer	Adam [30]
Learning Rate	1.0
Batch Size	8
Weight Decay	$1e^{-5}$
Maximum Sequence Length	512

Table 9: Finetuning hyperparameters for the classifiers in our text experiments.

Hyperparameter	Question Answering
Number of epochs	5 (discriminator), 3 (experts)
Learning rate	$5e^{-4}$
Optimizer	Adam
Dropout	0.1
Batch Size	8
Max Input Length	384
LoRA Rank	32
LoRA Alpha	32

D Additional Experiments

D.1 Additional Discriminator Comparisons

We present the results on the remaining datasets for domain discrimination, comparisons between the S-Prompts discriminator, our G2D discriminator, and an oracle discriminator trained on samples with ground truth domain identifiers. We observe that our discriminator outperforms the alternative approach on all tasks.

Table 10: We compare the performance of the G2D domain discriminator with the S-Prompts discriminator (that uses KMeans and KNNs). We also provide a comparison to a discriminator trained on real samples (Oracle Discriminator). The G2D discriminator outperforms the S-Prompts discriminator on all tasks.

Dataset	S-Prompts Disc.	G2D Disc. (ours)	Oracle Disc.
DomainNet	80.33 \pm 0.05	83.74 \pm 0.99	85.03 \pm 0.74
CORe50	90.81 \pm 0.27	97.38 \pm 0.93	98.94 \pm 0.07
DermCL	71.22 \pm 0.10	75.22 \pm 0.48	80.45 \pm 3.18

E Discussion on Generative Models in Healthcare

In general, and for good reason, practice in healthcare moves considerably slower than exploratory machine learning research. It is generally the case that ideas take root in the research community long before they show up in the clinic. Following this convention, due to the recency of successes of generative models (relative to discriminative models), contractual or regulatory requirements surrounding generative models is still in nascent stages of development.

What is the current status quo? The setting where model weights may be shared but not the actual training data is a well-known setting in the healthcare domain [28, 61, 64]. We elaborate on two examples: (1) Kamran et al. [28] presents a multisite external validation study for early identification of COVID-19 patients at risk of clinical deterioration, which require sharing the model trained on private EHR data from one US hospital with 12 other US medical centers; (2) Ulloa-Cerna et al. [61] presents a multisite external validation study for model development for identifying patients at increased risk of undiagnosed structural heart disease, which requires sharing the model trained on private EHR data and patient echocardiography reports from one site with 10 other independent sites. While these are generally examples of discriminative models being shared across facilities as opposed to generative models, this demonstrates the general principle that in such domains, model sharing is often permissible in settings where data sharing is not.

On one hand, it seems intuitive that healthcare institutions might be queasier about sharing generative models than sharing discriminative models. On the other hand,

- Healthcare institutions are even queasier about sharing real data — and to this end there is a large mainstream line of work investigating the use of generative models for direct sharing or for producing synthetic datasets that could be disseminated in lieu of actual patient data [8, 10, 18]
- From a standpoint of most contractual or regulatory requirements, it is not yet clear even if generative models sit in a different category than discriminative models or if they should follow the same current regulatory requirements for discriminative models.
- How institutional practices develop and the regulatory environment evolve will be informed, to a large degree, by exploratory research that characterizes both (i) the potential benefits and (ii) the potential risks associated with the dissemination of generative models trained on medical data.

F Example Generations

We include example generations for both image and text domains.

F.1 Examples of Generated Images











Class Label	Synthetic Images	Real Images
Aircraft Carrier		
Bicycle		
Birthday Cake		
Alarm Clock		
Ambulance		

Figure 3: Comparison of sampled synthetic images and real images from the DomainNet benchmark.

F.2 Examples of Generated Text

Table 11: Generated samples (context, question-answer pair) for the SQuAD domain. For the incorrectly generated samples, we underline one possible correct answer.

Dataset	Fields	Generated sample
SQuAD		Correct
	<i>Context:</i>	During the late 19th and early 20th centuries, the city’s trade sector expanded greatly, and through the 20th century, more than half of its residents worked toward higher status in the military. Other industries included industry, commerce, public administration, and medicine. Its largest sector was public services - police, fire services, and healthcare and was the nation’s third largest.
	<i>Question:</i>	What is one of the industry sectors that were the biggest?
	<i>Answer:</i>	public services
SQuAD		Incorrect
	<i>Context:</i>	In the United Kingdom there is a general agreement between the government and the private sector in principle that both private and publicly funded institutions of higher education constitute <u>university colleges</u> . Further, there is a mutual agreement between the <u>independent college</u> and the university to promote higher education. However, in both cases all the institutions of higher education are either controlled by private individuals or by a national agency, in such a way as to protect freedom of expression.
	<i>Question:</i>	What are some of the institutions of higher education that are controlled by private individuals?
	<i>Answer:</i>	private individuals